Journal of Catalysis **197,** 26–33 (2001)
doi:10.1006/jcat.2000.3068, available online at http://www.idealibrary.com on IDEAL®

# Correlation between Hydrodesulfurization Activity and Order of Ni and Mo Sulfidation in Planar Silica-Supported NiMo Catalysts: The Influence of Chelating Agents

L. Coulier, V. H. J. de Beer, J. A. R. van Veen, and J. W. Niemantsverdriet[1]

*Schuit Institute of Catalysis, Eindhoven University of Technology, P.O. Box 513, 5600 MB Eindhoven, The Netherlands*

Received March 8, 2000; revised September 13, 2000; accepted September 13, 2000

**Surface science models of silica-supported NiMo catalysts have been prepared to study the formation of the active phase ("NiMoS") in hydrotreating catalysts. Combination of XPS and thiophene hydrodesulfurization (HDS) measurements shows that the key step in the formation of the NiMoS phase is the order in which Ni and Mo precursors transfer to the sulfidic state. In NiMo systems prepared by conventional methods the sulfidation of Ni precedes that of Mo. However, complexing Ni to chelating agents like nitrilotriacetic acid, ethylenediamine, ethylenediaminetetraacetic acid (EDTA), and 1,2-cyclohexanediaminetetraacetic acid (CyDTA) retard the sulfidation of Ni. For EDTA and CyDTA the Ni sulfidation is delayed to temperatures where $MoS_2$ is already formed. These catalysts show the highest activity in thiophene HDS, indicating that complete sulfidation of Mo preceding that of Ni provides the ideal circumstances for NiMoS formation.** © 2001 Academic Press

*Key Words:* **model catalyst; sulfidation; XPS; nickel; molybdenum; silica; hydrodesulfurization; chelating ligands; thiophene.**

## INTRODUCTION

Catalysts used in the hydrotreating of oil fractions consist of sulfides of molybdenum or tungsten, promoted with cobalt or nickel supported on alumina. In catalysts based on molybdenum, the active phases are the so-called "CoMoS" and "NiMoS" phases, which consists of sulfided Co or Ni atoms decorating the edges of $MoS_2$ slabs (1–3).

Silica-supported CoMo catalysts, prepared by conventional impregnation from aqueous solutions of Co and Mo salts, exhibit low hydrotreating activity compared to the $\gamma$-$Al_2O_3$-supported catalysts (4, 5). This has been attributed to the low dispersion of Co and Mo after calcination and consequently to the low concentration of the active phase, caused by the weak interaction with the support (4, 5). Adding chelating agents, like nitrilotriacetic acid (NTA), and thereby leaving out the calcination step, proved to be a way of preparing hydrotreating catalysts on any support with similar hydrotreating activity as their $\gamma$-$Al_2O_3$-supported counterparts (4, 6).

Prins and coworkers (7–9) have shown that addition of chelating agents, such as NTA, ethylenediaminetetraacetic acid (EDTA), and ethylenediamine (ED) has a similarly favorable effect on high surface area NiMo/$SiO_2$ catalysts. TPS and EXAFS studies show that adding NTA to the impregnating solutions prevents the sulfidation of Ni at low temperature, thereby increasing the formation of the NiMoS phase, as was deduced from the increased activity in thiophene HDS (7). De Jong *et al.* (10) showed that the same effect, i.e., stabilization of cobalt against sulfidation, explains the role of NTA in enabling the formation of "CoMoS" in silica-supported CoMo catalysts. Shimizu *et al.* (11, 12) reported that adding chelating agents in the preparation also has a beneficial effect for the activity of $Al_2O_3$-supported HDS catalysts.

Model catalysts, consisting of a flat conducting substrate with a thin $SiO_2$ or $Al_2O_3$ layer on top of which the active phase is deposited, have been very successful in the field of catalysis research (13). The advantage of these model systems, having a conducting substrate, is that sample charging is largely eliminated, resulting in much better resolution of XP spectra with respect to high surface area catalysts (13). The model catalysts are prepared by spincoating (14), a technique mimicking the impregnation technique used for porous catalysts, which offers full control over the loading (15).

In this article $SiO_2$-supported NiMo model catalysts are used to study the formation of the active phase during sulfidation and the influence of various chelating agents. By comparing the stepwise sulfidation studied by semi-*in-situ* X-ray photoelectron spectroscopy and the thiophene HDS activity we show that the extent to which chelating agents retard the conversion of nickel to sulfides with respect to that of molybdenum correlates directly with the activity of the catalysts for thiophene HDS. A parallel comparison of the role of chelating agents on CoMoS formation in CoMo/$SiO_2$ catalysts has been published elsewhere (16).

[1] To whom correspondence should be addressed. Fax: 0031 40 245 5054. E-mail: j.w.niemantsverdriet@tue.nl.



0021-9517/01 $35.00

## EXPERIMENTAL

$NiMo/SiO_2/Si$ model catalysts were prepared in the same way as the CoMo system described in detail earlier (16). Briefly, a silica model support was prepared by oxidizing a Si(100) wafer in air at 750°C for 24 h. After oxidation the wafer was cleaned in a mixture of $H_2O_2$ and $NH_4OH$ at 65°C. The surface was rehydroxylated by boiling in water for 30 min. Next this model support was covered with the impregnation solution, containing the catalyst precursor compounds, and dry-spinned in a homemade spincoat apparatus in $N_2$ atmosphere with 2800 rpm. The catalyst precursors were nickel nitrate and ammonium heptamolybdate. The concentration of Ni and Mo were adjusted to obtain loadings of 2 Ni and 6 Mo atoms/nm$^2$ after spincoating, as calculated according to Ref. (15). After spincoating the catalysts were calcined in 20% $O_2$/Ar at 500°C for 60 min at a rate of 5°C/min. For comparison, uncalcined samples were measured as well; these will be indicated as NiMo-uncalc/$SiO_2$.

Catalysts containing chelating agents were prepared by spincoating the support with ammoniacal solutions containing $MoO_3$, nickel nitrate, and the chelating agent as described by Van Veen *et al.* (4). The amount of chelating agents was adjusted as to complex both Ni and Mo, except for ED, where a Ni : ED ratio of 1 : 4 was taken (8, 9). Chelating agents used were NTA (Acros Organics, 99%), EDTA (Merck, p.a.), ED (Fluka, p.a.) and cyclohexanediaminetetraacetic acid (CyDTA) (Fluka, p.a.). The notation NiMo–NTA/$SiO_2$/Si(100) refers to a catalyst to which NTA was added in the preparation.

Sulfidation of the catalysts was carried out in a glass tube reactor in 10% $H_2S/H_2$. The catalysts were heated at a rate of 5°C/min (chelating agents: 2°C/min) to the desired temperature and kept there for 30 min. After sulfidation, the reactor was cooled to room temperature under a helium flow and brought to the glovebox, where the model catalyst was mounted in a transfer vessel for transport to the XPS under $N_2$ atmosphere.

XPS spectra were measured on a VG Escalab 200 MK spectrometer equipped with an Al$K\alpha$ source and a hemispherical analyzer connected to a five-channel detector. Measurements were done at 20 eV pass energy. Energy correction was performed by using the Si 2*p* peak of $SiO_2$ at 103.3 eV as a reference. Binding energies were determined with a precision of ±0.2 eV. In a few cases a shift in binding energy of Ni and Mo was observed at high sulfidation temperature due to the increased conductivity of the sulfide phase. XPS spectra have been corrected for this.

Atmospheric gas-phase thiophene HDS was carried out in batch mode under standard conditions (1.5 bar, 400°C, 4% thiophene/$H_2$) after presulfidation at 400°C. For more details on the activity measurements, see (16).

## RESULTS

### *Sulfidation of Nickel and Molybdenum*

*$Ni/SiO_2$.* Figure 1 shows the Ni 2*p* XP spectra of a $Ni/SiO_2$ model catalyst, after sulfidation at various temperatures. The Ni 2*p* spectrum of the unsulfided catalyst shows the characteristic pattern of oxidic nickel with the Ni $2p_{3/2}$ peak at 856.8 eV and a shake-up feature at higher binding energy (17). The binding energy of 856.8 eV corresponds well with that of $Ni_2O_3$ (17). Sulfidation at room temperature shows the appearance of a second doublet at lower binding energy. At higher temperatures this doublet increases in intensity, while the doublet at 856.8 eV decreases and disappears at temperatures above 50°C. The Ni 2*p* doublet at 853.8 eV after sulfidation at high temperatures corresponds well with that of bulk nickel sulfide, $Ni_3S_2$ (17). The Ni 2*p* doublet of nickel sulfide also shows shake-up features at higher binding energy, but the intensity of the peaks is less than in the case of oxidic nickel. The S 2*p* spectra (not shown) confirm that the sulfidation starts already at room temperature and is completed at 100°C. Sulfidation of uncalcined $Ni/SiO_2$ and $Ni/SiO_2$ with different Ni loadings

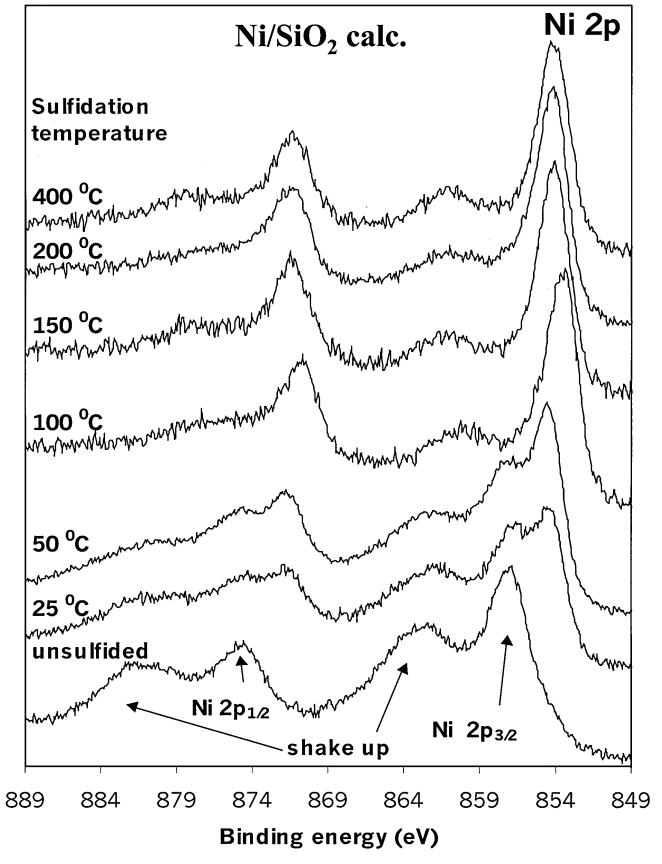


**FIG. 1.** Ni 2*p* XP spectra of $NiO/SiO_2/Si(100)$ model catalysts sulfided in 10% $H_2S/H_2$ for 30 min at various temperatures, showing that nickel oxide is already converted to bulk nickel sulfide at low temperatures.

yielded similar XP spectra as in Fig. 1. Complexing Ni to NTA retards the sulfidation of Ni by about 100°C as compared to calcined $Ni/SiO_2$. The binding energy of the fully sulfided Ni–NTA catalysts of 853.8 eV indicates that bulk nickel sulfide is formed at high sulfidation temperatures (see Table 2).

*$Mo/SiO_2$.* The sulfidation behavior of molybdenum was described extensively in earlier papers (10, 16, 18–21). Briefly, the sulfidation of Mo proceed at moderate temperatures, starting at around 50°C. Complete transformation to $MoS_2$ occurs at temperatures above 150°C. Note that these temperatures are significantly higher than for the sulfidation of $Ni/SiO_2$ in Fig. 1. The Mo 3*d* spectra of the catalysts sulfided at intermediate temperatures can be all interpreted in terms of $Mo^{6+}$, $Mo^{5+}$, and $Mo^{4+}$ doublets as described in an earlier paper (10, 18). Addition of chelating agents in the preparation stage did not affect the sulfidation behavior of Mo significantly, except for an almost 1-eV decrease in the binding energy of the unsulfided catalyst as compared to standard $MoO_3$ due to complexation (see the example of Mo–NTA in Table 1). Sulfidation of Mo at high temperatures leads to complete transition to $MoS_2$, as in $Mo/SiO_2$ without chelating agents.

*$NiMo/SiO_2$.* Figure 2 shows the Ni 2*p* and Mo 3*d* spectra of $NiMo/SiO_2$ in different stages of sulfidation. The Mo 3*d* spectra, shown in Fig. 2A, are identical to those of $Mo/SiO_2$ (16). However, the Ni 2*p* spectra in Fig. 2B reveal slower conversion of nickel to the sulfidic state than in $Ni/SiO_2$ (see Fig. 1). The sulfidation of Ni starts at temperatures around 100°C, which is 75°C higher than for the calcined $Ni/SiO_2$ catalyst. At these temperatures a second doublet with small shake-up features appears at a binding energy of 854.2 eV. Above 150°C the sulfidation is complete. The binding energy of the sulfided Ni is 0.4 eV higher than that of sulfided $Ni/SiO_2$. Comparing Ni and Mo, one observes that the rates of sulfidation are similar, with the start around 50°C and completion between 150° and 200°C.

The XP spectra of uncalcined $NiMo/SiO_2$ catalysts (not shown) are similar to those of the single-phase catalysts. Sulfidation of Ni precedes that of Mo, although the temperature regime where sulfidation occurs shows some overlap. Noteworthy is that the binding energy of sulfided Ni in uncalcined $NiMo/SiO_2$ equals that of the sulfided Ni-only catalysts.

### *Influence of Chelating Agents on the Sulfidation Behavior of Ni and Mo*

*$NiMo\text{-}EDTA/SiO_2$.* Figure 3 shows the Ni 2*p* and Mo 3*d* spectra of a NiMo–EDTA/$SiO_2$ sulfided at various temperatures. The Mo 3*d* spectrum of the fresh catalyst shows one doublet with a binding energy of 232.2 eV characteristic of complexated molybdenum, as discussed above. The sulfidation behavior of Mo is identical to that of $Mo/SiO_2$ and $NiMo/SiO_2$, with conversion to sulfides starting around

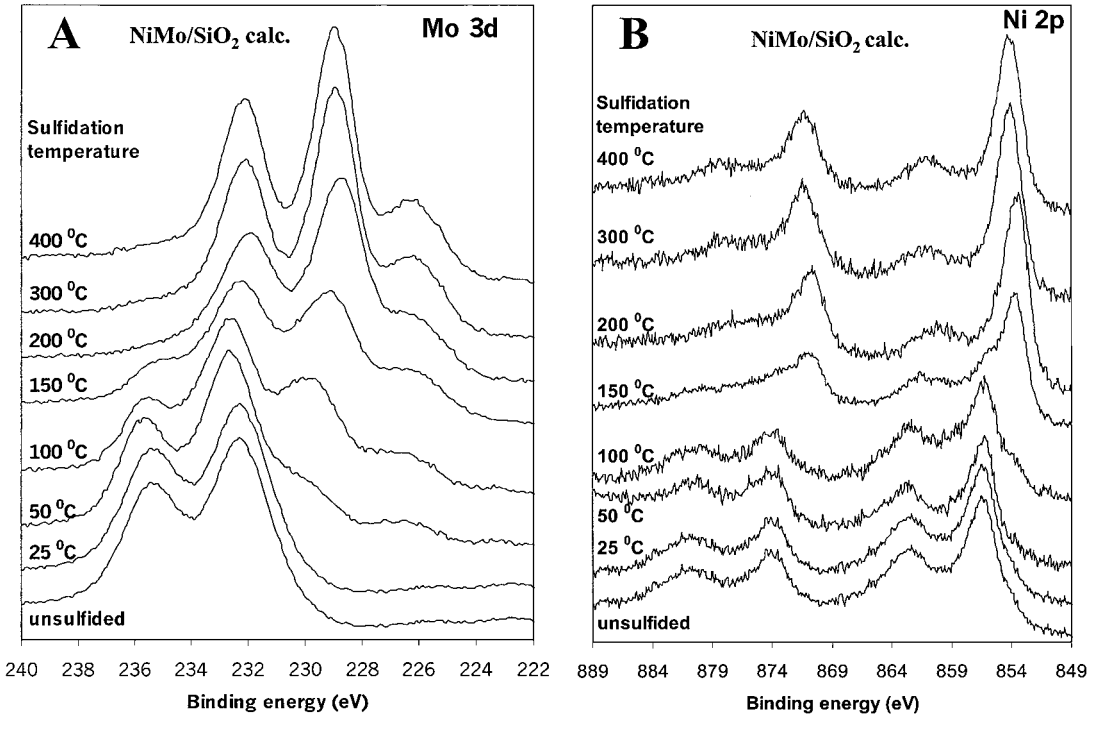


**FIG. 2.** (A) Mo 3*d* and (B) Ni 2*p* XP spectra of a calcined $NiO/MoO_3/SiO_2/Si(100)$ model catalyst during sulfidation at different temperatures. The spectra show that the sulfidation of Ni is retarded due to a Ni–Mo interaction, resulting in simultaneous sulfidation of Ni and Mo.

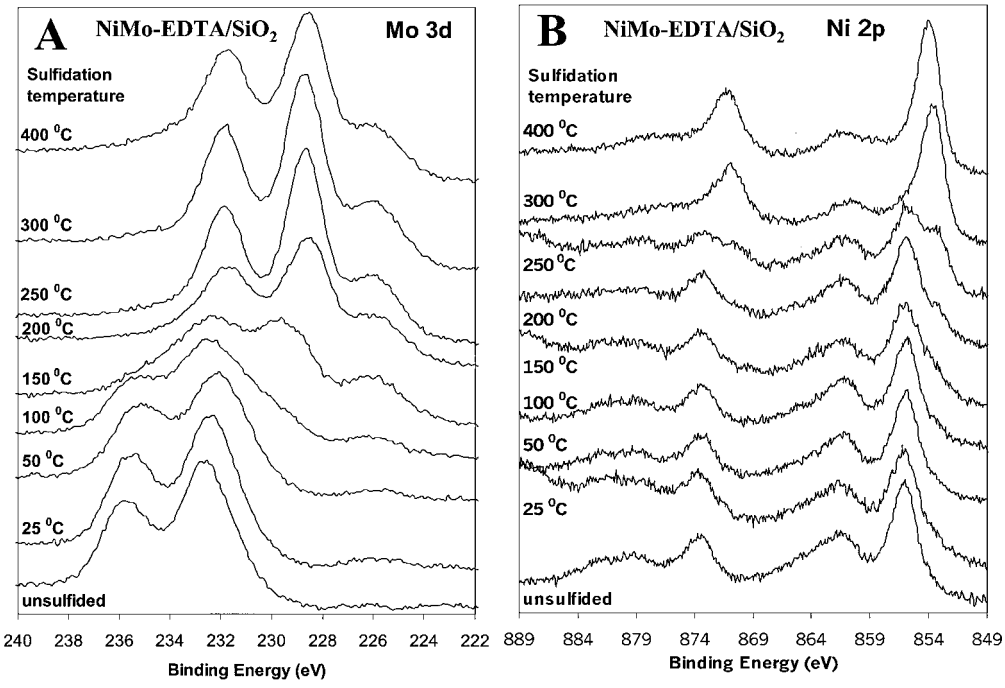


**FIG. 3.** (A) Mo 3*d* and (B) Ni 2*p* XP spectra of NiMo–EDTA/$SiO_2$/Si(100) model catalysts during sulfidation at different temperatures. The spectra show that EDTA retards the sulfidation of Ni even more, while Mo still sulfides at the same temperature. The sulfidation of Mo precedes that of Ni and both sulfide in separate temperature regimes.

50°C and being completed above 150°C. The single doublet at 229.0 eV is characteristic for $MoS_2$.

The Ni 2*p* spectra in Fig. 3B show that EDTA retards the sulfidation of Ni significantly. The spectrum of the fresh catalyst shows a single doublet at 856.1 eV, corresponding to Ni complexed to EDTA, and shake-up features at higher binding energy. Sulfidation does not start until temperatures around 200°C where a second doublet at lower binding energy appears. The sulfidation is complete at 300°C. Note that the binding energy of the sulfided Ni, 854.1 eV, is 0.3 eV higher than that of the fully sulfided Ni/$SiO_2$ catalysts at 853.8 eV.

Retardation of the sulfidation of Ni occurs when NTA is used as chelating agents, although the effect is not as strong as with EDTA. As a result, there exists some overlap in temperature regime in which Ni and Mo convert to the sulfidic state, whereas with EDTA Ni and Mo convert to sulfides in fully separated temperatures regions. The binding energy of the nickel in the sulfidic state (854.2 eV) equals that in NiMo–EDTA/$SiO_2$.

XPS studies on NiMo–CyDTA/$SiO_2$ catalysts revealed that CyDTA retards the sulfidation of Ni to even higher temperatures than EDTA does. The situation is very similar to that in the NiW–CyDTA system, as we published recently (22).

*NiMo-ED/$SiO_2$.* Figure 4 shows the effect of ED on the sulfidation of nickel in the Ni 2*p* and N 1*s* (containing also the Mo $3p_{3/2}$) spectra of NiMo–ED/$SiO_2$. The Mo 3*d* spectra are not shown because they are similar to that of NiMo/$SiO_2$ in Fig. 2B. The Ni $2p_{3/2}$ peak in the spectrum of the fresh catalyst has a binding energy of 856.0 eV (Table 1), which is significantly lower than that of oxidic Ni and therefore can be attributed to Ni complexed to ED. Sulfidation is revealed by the Ni 2*p* spectra, while the N 1*s* spectra monitor the presence of ethylenediamine in the catalyst. Sulfidation of Ni starts already at room temperature and appears to be complete at 100°C. The N 1*s* peak at 400 eV decreases in intensity but remains visible to temperatures up to 200°C, indicating that ethylenediamine is still present in small amounts. The Ni 2*p* binding energy is 853.8 eV after sulfidation up to 200°C but increases to 854.3 eV after sulfidation at 400°C. The sulfidation of Mo is completed above 150°C. Hence, the Ni sulfide assumes its final form at temperatures above those where Mo is fully sulfided.

**TABLE 1**

**XPS Binding Energies of Fresh NiMo/$SiO_2$ Catalysts**

| Catalyst prepared | Binding energy (eV) | |
|---|---|---|
| | Mo $3d_{5/2}$ | Ni $2p_{3/2}$ |
| Without chelating agents | 232.8 ± 0.2 | 856.6 ± 0.2 |
| With ethylene diamine (ED) | 232.5 ± 0.2 | 856.0 ± 0.2 |
| With nitrilo triacetic acid (NTA) or ethylenediamine tetraacetic acid (EDTA) | 232.2 ± 0.2 | 856.2 ± 0.2 |

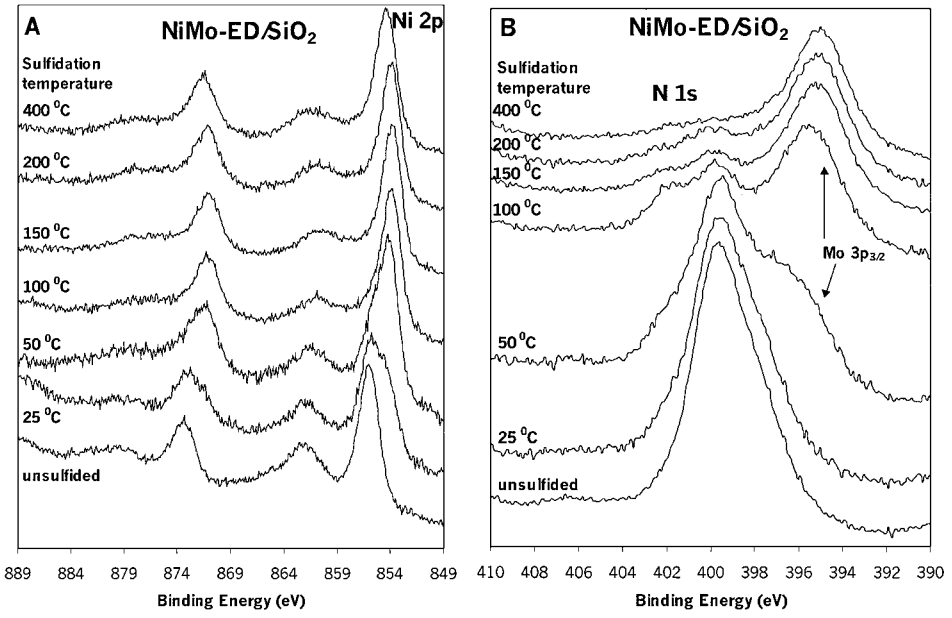


**FIG. 4.** (A) Ni 2*p* and (B) N 1*s* XP spectra of NiMo–EN/$SiO_2$/Si(100) model catalysts sulfided in 10% $H_2S/H_2$ for 30 min at various temperatures.

*HDS Activity Measurements*

Demonstrating that the planar model systems are catalytically active in hydrodesulfurization is the most convincing test for the validity of the model approach and enables us to make correlations between sulfidation and catalytic behavior. To this end, batch thiophene HDS activity measurements were performed on all model systems.

Figure 5 compares the activity of the different model catalysts in thiophene HDS discussed in this paper. The activity is expressed as yield of products per 5 $cm^2$ of catalyst after 1 h of batch reaction at 400°C and has been corrected for blank measurements (bare silica support and empty reactor).

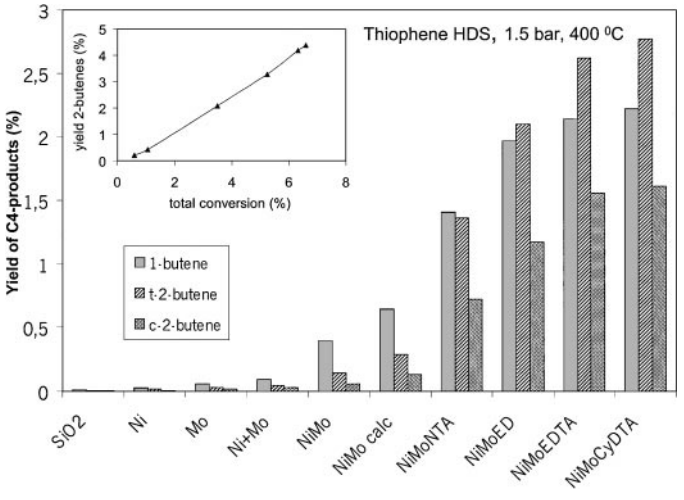


**FIG. 5.** Thiophene HDS product distributions measured for various $SiO_2$/Si(100) supported sulfided Ni, Mo, and NiMo catalysts (batch reaction at 400°C, runtime 1 h).

The activity of Ni/$SiO_2$ is low, although noticeably, and corresponds to a pseudo-turnover frequency of $1.8 \times 10^{-3}$ thiophene per Ni atom per second. Low activities were also found for uncalcined Ni/$SiO_2$ and Ni–NTA/$SiO_2$ (not shown). Mo/$SiO_2$ shows a somewhat higher activity than Ni/$SiO_2$, but the yield is still low (<0.5%). For Mo–NTA/$SiO_2$ the same activity was observed as for Mo/$SiO_2$. The synergistic effect of Ni and Mo is clearly visible from the large increase in activity of, e.g., NiMo/$SiO_2$ compared to Mo/$SiO_2$ calc. The activity of calcined NiMo/$SiO_2$ is higher than that of uncalcined NiMo/$SiO_2$, which we attribute to an increase in Ni–Mo interaction due to calcination, as will be explained in the discussion.

The highest activities are observed in NiMo/$SiO_2$ catalysts prepared with chelating agents, as Fig. 5 shows. The relative amount of secondary products, i.e. *t*-2-butene and *c*-2-butene, becomes appreciably higher than in the product distribution of the less active catalysts. The inset in Fig. 5 shows a selectivity plot of the total yield of 2-butenes (%) against the total conversion. The straight line confirms that the variations in product distribution observed with the different catalysts are caused by a kinetic effect. NiMo–EDTA/$SiO_2$ and NiMo–CyDTA/$SiO_2$, for which the sulfidation of Mo precedes that of Ni and sulfidation takes place in separate temperature regimes, appears to be the most active catalyst. The thiophene conversion into $C_4$-olefins is roughly a factor of 5 higher than that of the standard (i.e., calcined) NiMo/$SiO_2$ catalyst.

If we arrange the catalysts into groups with low, standard, and enhanced HDS activity, we find a correlation between

**TABLE 2**

**XPS Binding Energies of Sulfided NiMo/$SiO_2$ Catalysts**

| | Binding energy (eV) | |
|---|---|---|
| | Mo $3d_{5/2}$ | Ni $2p_{3/2}$ |
| Low HDS activity | | |
| Ni/$SiO_2$, Ni–NTA/$SiO_2$, Mo/$SiO_2$, Mo-NTA/$SiO_2$ | $228.9 \pm 0.2$ | $853.8 \pm 0.2$ |
| Standard HDS activity | | |
| NiMo–uncalc/$SiO_2$ | $228.9 \pm 0.2$ | $853.8 \pm 0.2$ |
| NiMo–calc/$SiO_2$ | $229.0 \pm 0.2$ | $854.0 \pm 0.2$ |
| Enhanced HDS activity | | |
| All catalysts prepared with chelating agents | $229.0 \pm 0.2$ | $854.2 \pm 0.2$ |

*Note.* NiMo–CyDTA was not measured.

HDS activity and state of Ni in the sulfided catalyst as expressed by the Ni $2p_{3/2}$ binding energy (see Table 2).

## DISCUSSION

The major conclusion from this work is that a clear correlation exists between the thiophene HDS activity of NiMo/$SiO_2$ model catalysts and the order in which the initially oxidic nickel and molybdenum convert into the sulfidic state during presulfidation in $H_2S/H_2$. Topsøe's CoMoS model (1–3), applied to the Ni–Mo system (NiMoS) offers a good basis for explaining the differences between the differently prepared catalysts dealt with in this paper. The structure of the NiMoS phase consists of sulfided nickel decorating $MoS_2$ slabs. The most favorable order for converting a mixture of nickel oxide and molybdenum oxide to the NiMoS phase would be to let molybdenum form $MoS_2$ slabs, after which nickel can decorate the most reactive sites of the $MoS_2$, viz. those situated at the edges. This reversed order of sulfidation is best realized in the systems where CyDTA and EDTA are used as ligands for nickel, and the corresponding catalysts yield the most active NiMo combinations for thiophene HDS.

Below, the relation between sulfidation and activity properties will be briefly discussed for all catalysts studied.

*Ni/$SiO_2$.* The Ni $2p$ spectra in Fig. 1A show that the sulfidation of Ni/$SiO_2$ calc. proceeds through oxygen–sulfur exchange. The transformation of nickel from the oxidic state to the sulfidic state is clearly visible from the shift in the binding energy to lower values (see also Table 1). The sulfidation starts already at room temperature and is completed around 100°C. Comparing the binding energy at high sulfidation temperatures with binding energies of reference compounds, it appears that most probably $Ni_3S_2$ is present (17).

It is known that bulk nickel sulfide has low activity for thiophene HDS (3), which is confirmed by the low activity shown in Fig. 5. As stated earlier, neither calcination nor the application of a higher nickel loading caused any measurable changes in sulfidation behavior of Ni. Sulfidation of these samples results in the formation of bulk nickel sulfide and yields catalysts with a low HDS activity (experiments not shown).

Chelating agents have no effect on the HDS activity of Ni/$SiO_2$. Although NTA retards the sulfidation of Ni, in the absence of Mo, bulk nickel sulfide forms and therefore the HDS activity of Ni–NTA/$SiO_2$ is of the same order as that of Ni/$SiO_2$, as we indeed observed.

*Mo/$SiO_2$.* As described earlier, the sulfidation of Mo takes place at moderate temperatures and through different intermediates (16, 18). The sulfiding mechanism proceeds by O–S exchange transforming oxidic Mo into $MoS_2$. In the intermediate temperature range $Mo^{5+}$ and oxysulfide species are present (20, 21). It is known that supported $MoS_2$ slabs are active in HDS, which agrees with the observed thiophene HDS activity (Fig. 5). No significant differences in activity were found between uncalcined and calcined Mo catalysts, as expected in view of their similar sulfidation behavior. The same is true for Mo–NTA/$SiO_2$. Although the fresh Mo–NTA catalyst contains Mo atoms complexed to NTA (see Table 1), sulfidation at high temperature will form $MoS_2$ slabs independent of the initial state of Mo.

*NiMo/$SiO_2$.* The Ni $2p$ and Mo $3d$ XP spectra of uncalcined NiMo/$SiO_2$ are similar to those of the single phase Ni and Mo catalysts. We therefore conclude that in an uncalcined catalyst the two elements Mo and Ni do not influence each other's sulfidation behavior. As a result, Ni sulfidation almost entirely precedes that of Mo, apart from some overlap. Hence, unless redispersion of nickel sulfide is invoked, at most only a minor part of the Ni atoms will be able to migrate to $MoS_2$ to form the NiMoS phase. The moderate increase in HDS activity of NiMo/$SiO_2$ compared to that of Mo/$SiO_2$ (see Fig. 5) is in agreement with these ideas.

Calcination NiMo/$SiO_2$ has a beneficial effect on the HDS activity of the sulfided system, as seen in Fig. 5. Interestingly, the XP spectra show that due to calcination Ni sulfidation is retarded to higher temperatures: it starts at 100°C (instead of 25°C in Ni/$SiO_2$) and is completed around 200°C (100°C in Ni/$SiO_2$; see Fig. 2). We attribute this to a Ni–Mo interaction, although no clear proof is available at present. We encountered the same situation in the case of CoMo/$SiO_2$ model catalysts (16). Comparison with XPS spectra of reference samples indicates that the presence of $NiMoO_4$, which has been suggested (23) to be an ineffective precursor of NiMoS formation, can be excluded. The interaction between Ni and Mo has consequences for the rate at which both components form sulfides. Although Mo sulfidation still lags behind that of Ni, there is a significantly larger temperature range where Ni and Mo sulfide simultaneously, with a greater chance to form the desired

NiMoS phase. This explains the higher activity of the calcined NiMo/$SiO_2$ catalyst.

*NiMo-NTA/$SiO_2$.* Adding NTA to the impregnating solution leads to complexation of Ni and stabilizes Ni against sulfidation, whereas Mo sulfidation is not affected by the NTA ligands. As a result the sulfidation of Mo now largely precedes that of Ni. This should be sufficient to enable formation of a relatively large amount of NiMoS phase. Indeed, the activity of sulfided NiMo-NTA/$SiO_2$, shown in Fig. 5, is rather high. In earlier publications the same effect of NTA was observed for CoMo/$SiO_2$ model catalysts (10, 16).

The high activity of sulfided NiMo–NTA/$SiO_2$ is in agreement with the work of Prins and coworkers (7–9). These authors concluded from EXAFS data that NTA retards the sulfidation of Ni. However, differently as in our work, they found that Ni sulfidation still precedes that of Mo. We wonder if the difference may be due to the rate of $H_2O$ removal, which is extremely efficient in the present planar model catalysts, but is considerably slower in porous catalysts. According to Arnoldy *et al.* (24) and Weber *et al.* (21), sulfur uptake by the oxide proceeds by oxygen–sulfur exchange according to the reaction

$$MO_n + H_2S = MO_{n-1}S + H_2O.$$

Hence, a higher partial pressure of $H_2O$ in the pores of a high surface area catalyst will slow the sulfidation reaction down. Medici and Prins (7) also used a higher heating rate during sulfidation, which can also influence the sulfidation behavior of Ni and Mo. The difference in HDS activity between NiMo/$SiO_2$ and NiMo–NTA/$SiO_2$ is in our case much larger than that found by Prins *et al.* (7, 8). This suggests that the present planar models derived from NiMo–NTA/$SiO_2$ contain more Ni in the NiMoS phase than the corresponding high surface area catalysts used in (7, 8).

*NiMo-ED/$SiO_2$.* The complexation of ED to Ni in NiMo/$SiO_2$ catalysts was also studied by Prins *et al.* (8, 9). The authors found that a high Ni/ED ratio was required to complex all Ni. Using EXAFS they showed that the Ni–ED complex decomposes at low temperature, resulting in the sulfidation of Ni at low temperatures (8, 9). Nevertheless, the authors found a relatively high activity in thiophene HDS.

The XP spectra of NiMo–ED/$SiO_2$ model catalysts in Fig. 4 show that indeed a major part of Ni–ED complexes decomposes at low temperatures, resulting in the sulfidation of Ni at low temperatures. However, the N 1*s* spectra indicate that not all ED disappears at low temperatures. A small N 1*s* peak at 400 eV remains visible up to temperatures above 200°C, but has disappeared after sulfidation at 400°C. At the same temperatures the binding energy of the Ni 2*p* peak shifts from 853.8 to 854.4 eV, demonstrating that the structure of the nickel sulfide changes above 200°C.

We propose the following picture. It is known that Ni complexes to more than one ED molecule (8, 9). At low temperatures most of these ED ligands disappear and Ni sulfides partially, but remains attached to at least one ED molecule. The last ED ligand disappears at high temperatures and releases the partially sulfided Ni. Because Mo is already completely sulfided at these temperatures, the now completely sulfided Ni is able to migrate to the $MoS_2$ edges, thereby forming NiMoS. The observed perseverance of the N 1*s* signal up to at least 200°C, the change in binding energy of sulfidic Ni above this temperature, and the high activity of fully sulfided NiMo–ED/$SiO_2$ support this idea.

*NiMo-EDTA/$SiO_2$.* EDTA, known to form very stable complexes with ions of nickel and cobalt (25), and the even more stable cyclohexane variant of this complex, CyDTA, are the most successful chelating agents with respect to stabilizing nickel against sulfidation in this study. Whereas Mo sulfidation is identical to that of Mo/$SiO_2$, the sulfidation of Ni is effectively retarded to temperatures above 200°C. Hence, all Mo is present as $MoS_2$ when the sulfidation of Ni starts. It is therefore expected, considering the relatively low Ni/Mo ratio (i.e., 1/3), that all Ni atoms are able to migrate to the edges of the $MoS_2$ slabs, thereby forming a maximum amount of NiMoS phase.

The HDS activity measurements in Fig. 5 show that the NiMo–EDTA/$SiO_2$ and NiMo–CyDTA/$SiO_2$ are indeed the most active catalysts. The activity is almost two times higher than that of NiMo–NTA/$SiO_2$. This is in qualitative agreement with Prins *et al.* (7–9), who also found that EDTA containing catalysts show higher activity than catalysts containing NTA. However, they reported a much smaller difference in HDS activity between EDTA- and NTA-containing catalysts. In a Quick EXAFS study on NiMo/$SiO_2$ catalysts, Cattaneo *et al.* (9) showed that EDTA retards the sulfidation of Ni, although Mo sulfides at higher temperatures than in our work. As a result Ni and Mo do not sulfide in separate regimes. This can explain the relatively small difference in HDS activity between NiMo–EDTA and NiMo–NTA catalysts in their study, compared to the results presented here, where Ni and Mo sulfide in separate regimes. Similarly as discussed above, it is proposed that sulfidation in porous catalysts is hindered by a slower removal of the reaction product $H_2O$, which is not a limiting factor in planar model catalysts.

We believe that retardation of Ni sulfidation with respect to that of Mo is the major reason for the activity enhancement observed in HDS. However, the XPS binding energies of Ni in fully sulfided catalysts from the high activity group are the same, and the XP spectra of the least active catalysts in this category, such as calcined NiMo/$SiO_2$ contain little evidence for the presence of Ni in more than one state. Hence, we cannot exclude that the chelating agents have some effect on the dispersion of $MoS_2$ particles as well. Unfortunately, the lack of reliable methods for determining

the edge dispersion of promoted sulfide particles prevents us from addressing this question satisfactorily.

## CONCLUSION

XPS measurements of the rate of sulfidation of Ni and Mo in a series of differently prepared silica-supported NiMo model catalysts have been correlated with the activity of these catalysts in thiophene hydrodesulfurization. Using standard impregnation from aqueous solutions of suitable nickel and molybdenum salts produces catalysts in which nickel converts more rapidly to the sulfidic state than molybdenum does. This produces catalysts of detectable but low activity in thiophene HDS. Adding chelating ligands such as NTA, EDTA, ED, or CyDTA stabilizes nickel against sulfidation at low temperatures and retards sulfidation of nickel to temperatures at which an appreciable amount of molybdenum is already in the form of $MoS_2$. As a consequence, such systems are believed to contain a relatively large fraction of nickel in the NiMoS form, consisting of $MoS_2$ with Ni decorating the edges. A maximum in HDS activity is obtained for systems in which the sulfidation of nickel is retarded to temperatures where Mo is completely sulfided. Retarding the sulfidation of Ni to higher temperatures does not enhance the activity; hence the complete sulfidation of Mo preceding that of Ni is the optimum condition for NiMoS formation.

## REFERENCES


1. Topsøe, H., and Clausen, B. S., *Catal. Rev.-Sci. Eng.* **26**, 395 (1984).
2. Prins, P., Beer, V. H. J. de, and Somorjai, G. A., *Catal. Rev.-Sci. Eng.* **31**, 1 (1989).
3. Topsøe, H., Clausen, B. S., and Massoth, F. E., "Hydrotreating Catalysis." Springer-Verlag, Berlin, 1996.
4. Veen, J. A. R. van, Gerkema, E., Kraan, A. M. van der, and Knoester, A., *J. Chem. Soc. Chem. Commun.* **22**, 1684 (1987).
5. Thompson, M. S., European patent application 0.181.035.A2 (1986).
6. Bouwens, S. M. A. M., Zon, F. B. M. van, Dijk, M. P. van, Kraan, A. M. van der, Beer, V. H. J. de, Veen, J. A. R. van, and Koningsberger, D. C., *J. Catal.* **146**, 375 (1994).
7. Medici, L., and Prins, R., *J. Catal.* **163**, 38 (1996).
8. Cattaneo, R., Shido, T., and Prins, R., *J. Catal.* **185**, 199 (1999).
9. Cattaneo, R., Weber, Th., Shido, T., and Prins, R., *J. Catal.* **191**, 225 (2000).
10. Jong, A. M. de, Beer, V. H. J. de, Veen, J. A. R. van, and Niemantsverdriet, J. W., *J. Phys. Chem.* **100**, 17722 (1996).
11. Shimizu, T., Hiroshima, K., Honma, T., Mochizuki, T., and Yamada, M., *Catal. Today* **45**, 271 (1998).
12. Ohta, Y., Shimizu, T., Honma, T., and Yamada, M., *Stud. Surf. Sci. Catal.* **127**, 161 (1999).
13. Gunter, P. L. J., Niemantsverdriet, J. W., Ribeiro, F. H., and Somorjai, G. A., *Catal. Rev.-Sci. Eng.* **39**, 77 (1997).
14. Kuipers, E. W., Laszlo, C., and Wieldraaijer, W., *Catal. Lett.* **17**, 71 (1993).
15. Hardeveld, R. M. van, Gunter, P. L. J., IJzendoorn, L. J. van, Wieldraaijer, W., Kuipers, E. W., and Niemantsverdriet, J. W., *Appl. Surf. Sci.* **84**, 339 (1995).
16. Coulier, L., Beer, V. H. J. de, Veen, J. A. R. van, and Niemantsverdriet, J. W., *Topics in Catal.* **13**, 99 (2000).
17. Moulder, J. F., Stickle, W. F., Sobol, P. E., and Bomben, K. D., "Handbook of XPS." Perkin Elmer Corporation, Eden Prairie, MN, 1992.
18. Jong, A. M. de, Borg, H. J., IJzendoorn, L. J. van, Soudant, V. G. M. F., Beer, V. H. J. de, Veen, J. A. R. van, and Niemantsverdriet, J. W., *J. Phys. Chem.* **97**, 6477 (1993).
19. Muijsers, J. C., Weber, Th., Hardeveld, R. M. van, Zandbergen, H. W., and Niemantsverdriet, J. W., *J. Catal.* **157**, 698 (1995).
20. Weber, Th., Muijsers, J. C., and Niemantsverdriet, J. W., *J. Phys. Chem.* **99**, 9194 (1995).
21. Weber, Th., Muijsers, J. C., Wolput, J. H. M. C. van, Verhagen, C. P. J., and Niemantsverdriet, J. W., *J. Phys. Chem.* **100**, 14144 (1996).
22. Kishan, G., Coulier, L., de Beer, V. H. J., van Veen, J. A. R., and Niemantsverdriet, J. W., *J. Chem. Soc. Chem. Commun.* 1103 (2000).
23. Scheffer, B., Jonge, J. C. M. de, Arnoldy, P., and Moulijn, J. A., *Bull. Soc. Chim. Belg.* **93**, 751 (1984).
24. Arnoldy, P., Heijkant, J. A. M. van de, Bok, G. D. de, and Moulijn, J. A., *J. Catal.* **92**, 35 (1985).
25. Silen, L. G., and Martell, A. E., "Stability Constants of Metal-Complexes," Vol. 2. Chemical Society, London, 1964.